Article

Mechanism and Selectivity of Rhodium-Catalyzed 1:2 Coupling of Aldehydes and Allenes

Genping Huang, Marcin Kalek, and Fahmi Himo

J. Am. Chem. Soc., **Just Accepted Manuscript** • DOI: 10.1021/ja4014166 • Publication Date (Web): 25 Apr 2013

Mechanism and Selectivity of Rhodium-Catalyzed 1:2 Coupling of Aldehydes and Allenes

Genping Huang, Marcin Kalek, and Fahmi Himo*

Department of Organic Chemistry

Arrhenius Laboratory

Stockholm University

SE-106 91 Stockholm, Sweden

Corresponding author: himo@organ.su.se

Abstract

The rhodium-catalyzed highly regioselective 1:2 coupling of aldehydes and allenes is investigated by means of density functional theory calculations. Full free energy profiles are calculated and several possible reaction pathways are evaluated. It is shown that the energetically most plausible catalytic cycle is initiated by the oxidative coupling of the two allenes, which is found to be the rate-determining step of the overall reaction. Importantly, Rh-allyl complexes that are able to adopt both η^3 and η^1 configurations are identified as key intermediates present throughout the catalytic cycle with profound implications on the selectivity of the reaction. The calculations reproduce and rationalize the experimentally-observed selectivities and provide explanation for the remarkable alteration in the product distribution upon changing the catalyst precursor from $[RhCl(nbd)_2]_2$ to complexes containing non-coordinating counterions ($[Rh(cod)_2X]$, X = OTf, BF_4, PF_6). It turns out that the overall selectivity of the reaction is controlled by a combination of the inherent selectivities of several of the elementary steps, and that both the mechanism and the nature of the selectivity-determining steps change when changing catalysts.

1. Introduction

Rhodium(I) complexes are well-established catalysts for the three-component cycloadditions of unsaturated compounds, yielding carbocycles with various ring sizes (for instance 6-membered, Scheme 1a).[1] Rhodium(I) also catalyzes hydroacylation reactions in which an acyl unit and the hydrogen atom of an aldehyde are added across a C-C multiple bond (Scheme 1b).[2] A reductive version of the latter process, furnishing the corresponding alcohols, has also been developed (Scheme 1c).[3] In 2006 Krische et al. reported a novel reaction that can be considered as a crossover between those presented in Scheme 1a and 1c. In its course, two molecules of acetylene are coupled with one molecule of aldehyde, under hydrogen atmosphere, forming a linear allylic alcohol product (Scheme 2a).[4,5] Very recently, a combination of the in principle more fundamental couplings from Schemes 1a and 1b has also been successfully accomplished.[6,7] In particular, a significant example comes from the laboratory of Murakami and consists of a 1:2 coupling of aldehydes and allenes (Scheme 2b).[6]

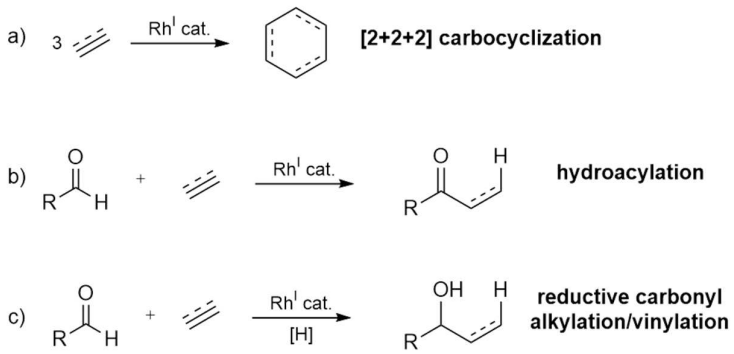

Scheme 1.

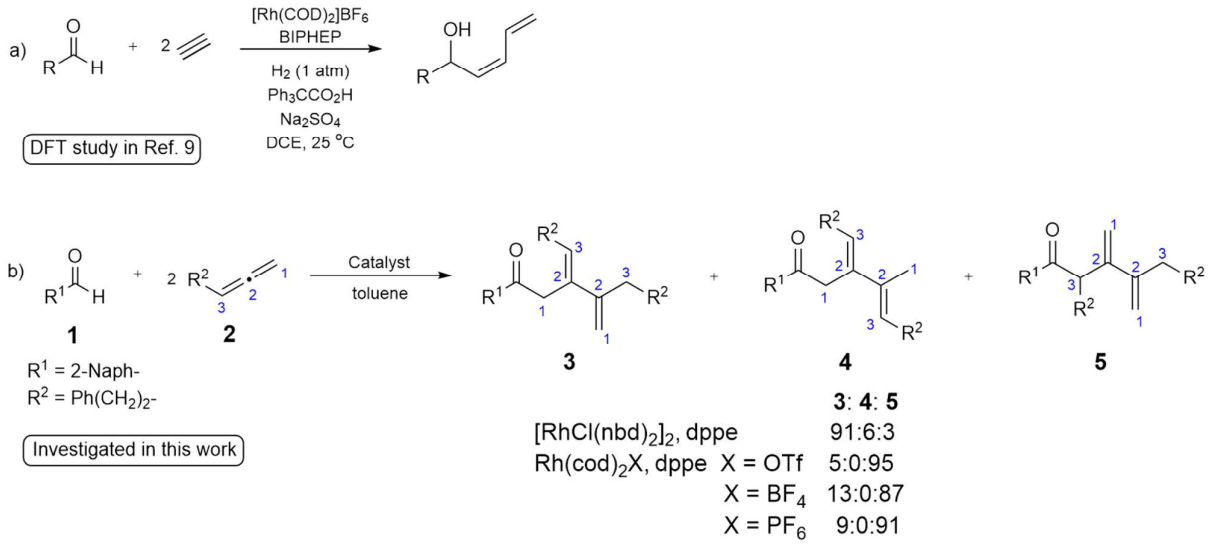

Scheme 2.

The reaction in Scheme 2b constitutes indeed a state-of-the-art method in synthetic organic chemistry. It is inherently atom-economical and leads to a large increase of molecular complexity in a single step. A particularly appealing feature of this process is its selectivity, which is a much more complex issue than in the reaction involving acetylene (Scheme 2a). Considering only the couplings of two monosubstituted allene moieties of type **2** with one molecule of aldehyde **1**, there are 36 different possible isomers of the product, with various connectivities and (*Z*)/(*E*) arrangements of the double bonds.[8] Experimentally, using $[RhCl(nbd)_2]_2$ as the rhodium source and dppe as the ligand, product **3** is obtained in 91% selectivity, accompanied by two minor isomers, **4** and **5** (6% and 3%, respectively).[6] Very interestingly, when the chloride is replaced by non-coordinating counterions, such as TfO^-, BF_4^-, or PF_6^-, the selectivity of the reaction is switched, and compound **5** becomes the dominant product (87-95%).[6] The common feature of the products obtained under both sets of the reaction conditions is that the two allene moieties are coupled with their central atoms (C2-C2 linkage) and the aldehyde is attached to one of the terminal carbons (C1 or C3) of one of

the allenes.

The reaction mechanism of the related three-component reductive coupling shown in Scheme 2a has been investigated by a combination of experimental and computational approaches.[9] It was established the reaction takes place via an initial oxidative coupling of two acetylene molecules, followed by migratory insertion of the aldehyde molecule, hydrogenolysis, and reductive elimination.[9] Hence, except for the extra hydrogenolysis step, this mechanism is similar to the well-established catalytic cycle of the trimerization process depicted in Scheme 1a.[1d]

In the case of the 2:1 coupling of allenes and aldehydes (Scheme 2b), it is not evident that an analogous mechanistic pathway is followed. It has been shown experimentally that allenes of type **2** indeed undergo an initial oxidative coupling in the presence of Rh(I) catalyst, but instead of the subsequent migratory insertion that would eventually result in the regular [2+2+2] cycloaddition (Scheme 1a), a β-hydride elimination/reductive elimination sequence occurs, leading overall to a linear dimer.[10,11] Additionally, it is known that the hydroacylation reactions (Scheme 1b) are initiated by an oxidative addition of aldehydes to Rh(I) complexes,[2a] hence this process may also be involved in the mechanism of the combined reaction shown in Scheme 2b. Finally, there is also an additional possibility of an initial oxidative coupling between the aldehyde and the allene moieties that has been shown to take place in some catalytic cycles.[12] A mechanism starting with the oxidative coupling of aldehyde and allene was actually suggested by Murakami and co-workers in their report.[6]

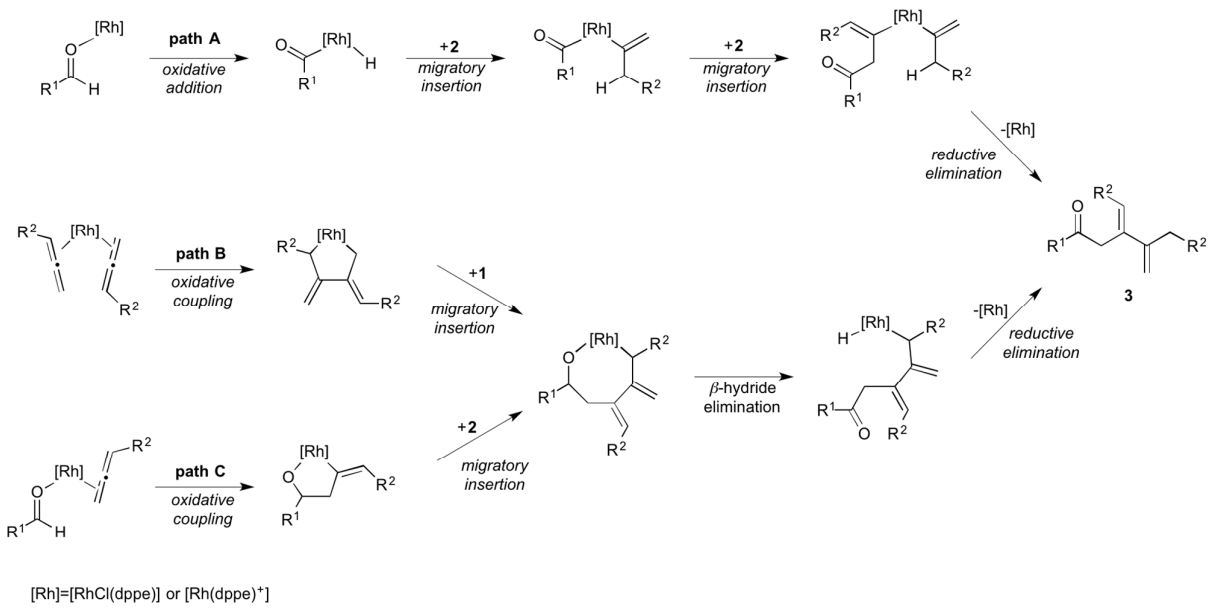

Scheme 3. Possible general mechanistic pathways for the reaction in Scheme 2b as suggested by experimental findings or proposed in the literature. Note that all pathways can yield all possible products. Here, only the routes leading product **3** are shown.

These possible mechanisms for the reaction, suggested by the experimental findings or proposed in the literature, are summarized in Scheme 3. They differ by the initial step, being C-H oxidative addition, allene-allene oxidative coupling, or aldehyde-allene oxidative coupling. In addition to the general mechanism there is the issue of the reaction selectivity and its sources. Each of the pathways shown in Scheme 3 may yield all of the 36 isomers of product, including the experimentally observed **3**, **4**, and **5**, by simply altering the positions at which the new bonds are formed. Moreover, all three pathways are consistent with the results of deuterium labeling studies carried out experimentally.[6] In addition, for almost all intermediates in Scheme 3 one can envision alternative reactions that they may undergo, not shown in the scheme, leading to side-products with entirely different structures (for instance **1-2** or **2-2** dimers, etc.), which adds to the complexity of

the system.

Considering the significance of the coupling reaction depicted in Scheme 2b and the current poor understanding of its mechanism, in particular the origins of the observed selectivity, we decided to investigate it computationally by means of density functional theory (DFT). The calculations show that the reaction indeed initially follows the pathway starting with the oxidative coupling of two allene molecules (Scheme 3, path B). However, we found that a previously not suggested allylation of aldehyde takes place subsequently with important selectivity implications. It is shown that a key role in the reaction mechanism is played by rhodium complexes containing allyl ligands, that adopt either η^3 or η^1 coordinations, displaying intrinsically distinct reactivities. Moreover, it is demonstrated that in the case of the reaction catalyzed by rhodium complexes with the non-coordinating counterions, a partially different mechanistic route is followed, involving an alkoxide oxidation step. The calculations provide an explanation for the observed selectivity switch upon altering the counterion in the Rh-catalyst.

2. Computational Details

All the calculations were performed using the Gaussian03 package[13] and the B3LYP functional[14]. Geometry optimizations were done with a combined basis set, in which Rh was described by the LANL2DZ basis set with pseudopotential,[15] and the 6-31G(*d*,*p*) basis set was used for all other atoms. Frequencies were computed analytically at the same level of theory to confirm whether the structures are minima (no imaginary frequencies) or transition states (only one imaginary frequency). Selected transition state structures were confirmed to connect the correct reactants and

products by intrinsic reaction coordinate (IRC) calculations. To obtain a better accuracy of the final energy values, energies were recalculated for the optimized geometries using single-point calculations with a larger basis set, that is LANL2DZ for Rh and 6-311+G(*2d*,*2p*) for the other atoms. The effect of solvation was evaluated by performing single-point self-consistent reaction field calculations with the conductor-like polarizable continuum model (C-PCM),[16] as implemented in Gaussian03. The parameters for toluene (ε = 2.379), corresponding to the experimental conditions, and the UAO radii were used in these calculations.

The final Gibbs energies reported in the article (ΔG_{Tol}) are the large basis set single-point energies corrected by Gibbs energy corrections (at 298.15 K), solvation corrections, and dispersion effects using the method of Grimme.[17] Adding the dispersion effects has recently been proven to significantly improve the performance of the B3LYP method.[18]

The calculations were carried out using the full structure of the 1,2-bis(diphenylphosphine)ethane (dppe) ligand, while the aldehyde and allene reactants were represented with smaller model structures, namely benzaldehyde (**1**, R^1=Ph in Scheme 2b) and buta-1,2-diene (**2**, R^2=Me), respectively.

3. Results and Discussion

Due to the number of possible mechanistic pathways (Scheme 3), the reaction poses a considerable challenge from a computational point of view. In this section, we first focus on the [RhCl(dppe)]-catalyzed reaction, assuming that chloride is coordinated to the metal center. The mechanism of the reaction is systematically examined step by step, by evaluating all the possible

pathways, including potential side-reactions. After the overall mechanism is established, the full catalytic cycle and the energy profile are summarized and the origins of the regioselectivity are discussed. In the final part, we present the results of the calculations on the reaction catalyzed by the cationic [Rh(dppe)$^+$] complex that is the putative active species in the reactions in which catalyst precursors containing the non-coordinating counterions are used. The obtained free energy profile is then analyzed and the origins of the observed alteration of the selectivity upon changing the catalyst are explained.

All energies are reported relative to the sum of the energies of the free reactants and catalyst (i.e. **1** + 2×**2** + [Rh], [Rh] = [RhCl(dppe)] or [Rh(dppe)$^+$]), which we have chosen to set to zero.

3.1. Initial step of the catalytic cycle – oxidative coupling vs. oxidative addition.

Before considering the various reaction pathways, we evaluated the different binding modes between the catalyst and the reactants. The calculations show that coordination of the allene (**2**) to the Rh catalyst (resulting in **INT1**, Figure 1) is exergonic by 8.9 kcal/mol, whereas binding of the aldehyde (**1**) is exergonic by 1.6 kcal/mol (**INT1a**, Figure 1). Introduction of any additional ligands always resulted in an increase in the free energy, which is in agreement with the known preference of d^8 metal complexes to adopt a four-coordinate square-planar geometry (see Supporting Information). Hence, **INT1** containing a single allene molecule, dppe, and chloride as ligands (see Figure 2 for structure) is the lowest energy Rh(I) species, to which the barriers for the initial step should be related.

As shown in Scheme 3, there are three general mechanistic pathways possible for the investigated reaction, each of which begins with a different step, namely: C-H oxidative addition

(path A), allene-allene oxidative coupling (path B), or aldehyde-allene oxidative coupling (path C). We have optimized the transition states corresponding to these steps and compared them in terms of their relative energies, taking into account all the possible coupling patterns of the reactants, where applicable.

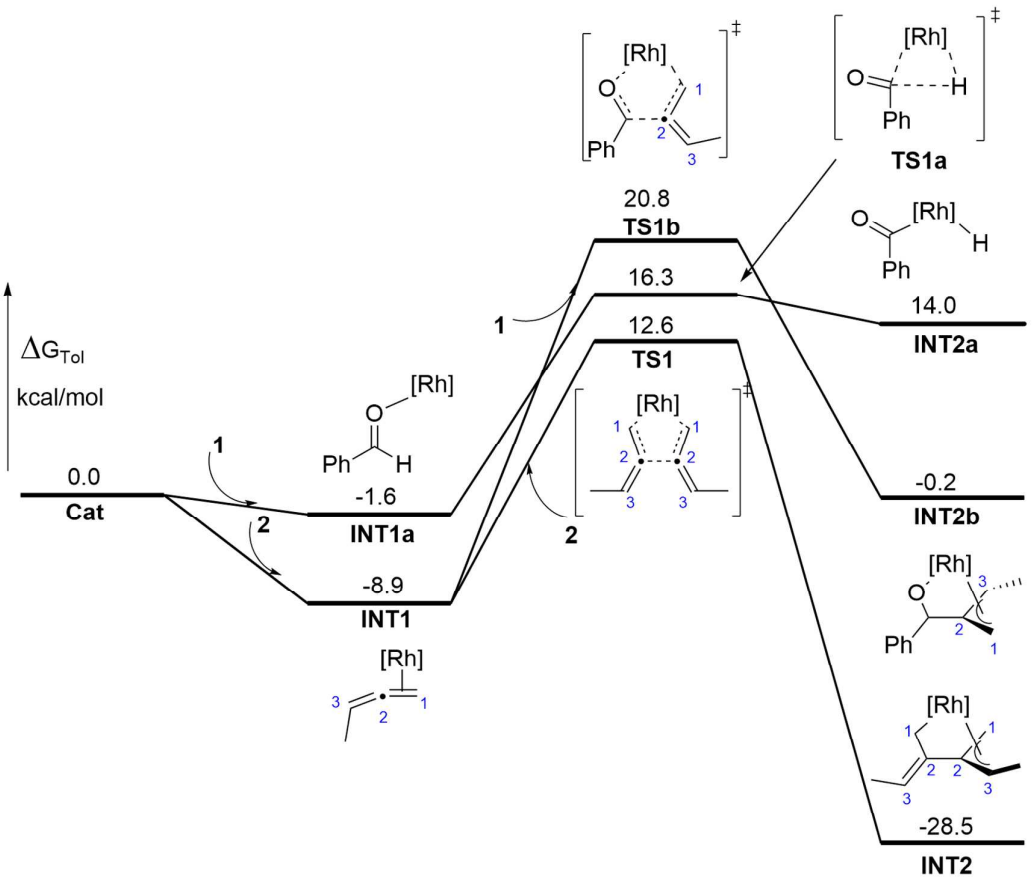

Figure 1. Free energy profile for the possible initial step of the reaction. The intermediates connecting **INT1** with **TS1** and **TS1b** are found to be higher in energy than **INT1**, hence they are not shown in the energy diagram (see Supporting Information for details).

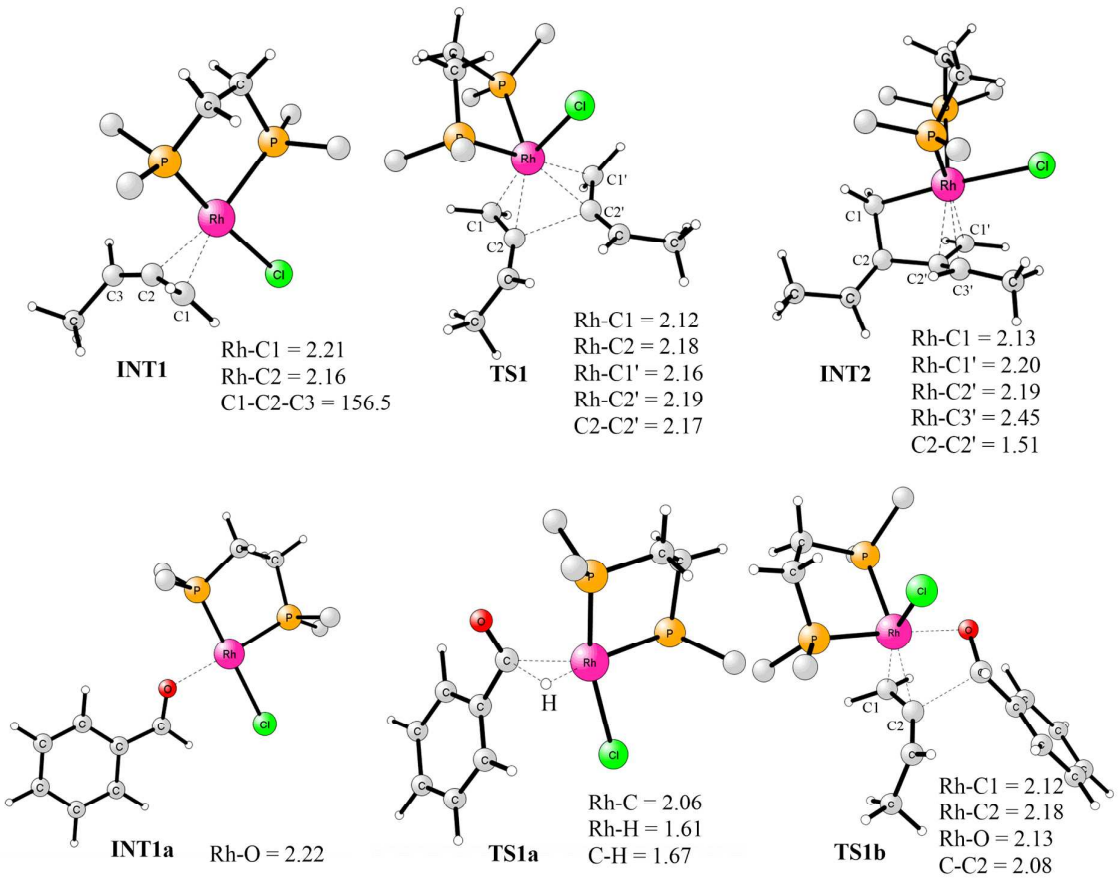

Figure 2. Optimized structures of selected intermediates and transition states for the initial step (distances in Å and angles in degrees). For clarity, the phenyl substituents on the phosphorus centers are omitted in the figure.

The C-H oxidative addition of aldehyde (path A in Scheme 3) was found to take place via transition state **TS1a** (Figure 2). It requires overcoming an overall barrier of 25.2 kcal/mol relative to **INT1**, and involves an initial interconversion into the aldehyde-containing complex **INT1a** (Figure 1). The oxidative addition results in the formation of the Rh(III) hydride **INT2a**, and the process is endergonic by as much as 22.9 kcal/mol.

The oxidative coupling of two allene moieties (path B in Scheme 3) is much more complicated to investigate than the oxidative addition. In the course of this step, the C-C bond formation may

occur between any of the three carbon atoms of each of the coupling partners (C1-C1, C1-C2, C1-C3, etc.). Additionally, when the central atom of the allene (C2) is engaged in the C-C bond formation, extra combinations arise from the fact that either of the terminal carbons (C1 or C3) may bind to the rhodium center. Taking into account also the (*Z*)/(*E*) arrangements of the double bonds and, in three cases, the *cis*/*trans* isomers, there are in total 24 possible distinct transition states that must be considered (Scheme 4). The energies for all of these were calculated, and the lowest one was found to be **TS1**, whose structure is shown in Figure 2 (structures and energies of all TSs are given in Supporting Information). In this TS, the rhodium center, which constitutes the largest steric bulk in the system due to the proximity of the phenyl-substituted phosphine ligand, is coordinating to the least substituted carbons (C1) of the allenes. Additionally, the (*Z*),(*Z*)-arrangement of the double bonds minimizes the repulsion in the other part of the structure. The free energy of **TS1** is calculated to be 21.5 kcal/mol relative to **INT1** (Figure 1). The energies of the other TSs shown in Scheme 4 are calculated to be higher than that of **TS1** by at least 2.2 kcal/mol (see Supporting Information).

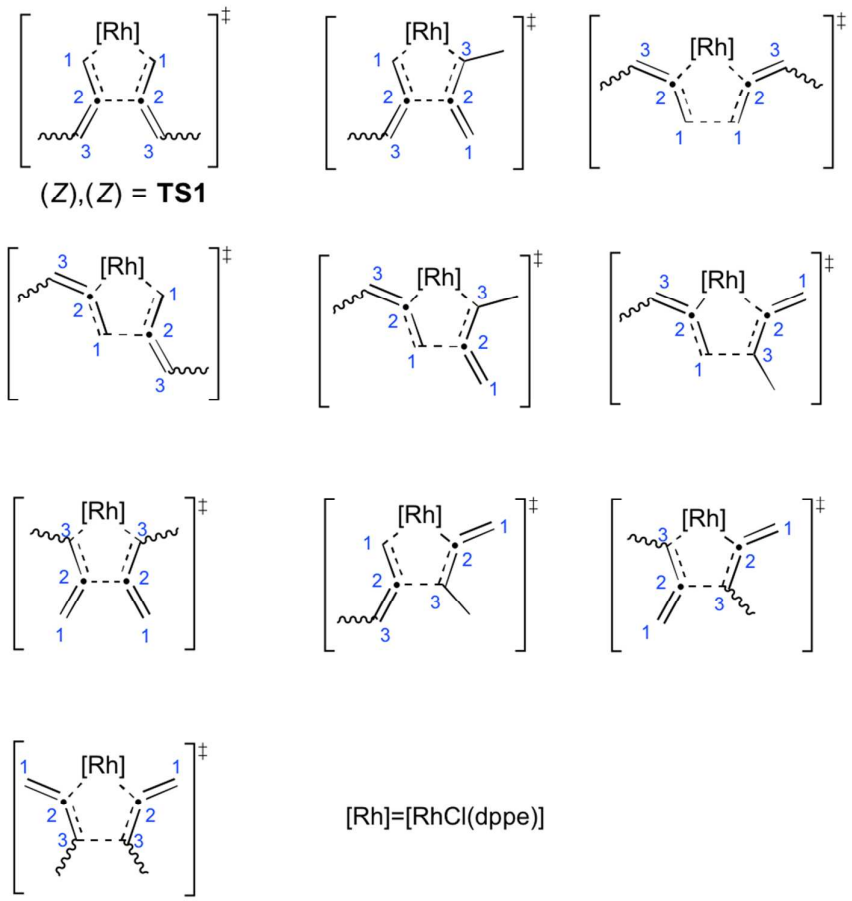

Scheme 4. Possible transition states for the oxidative coupling of the two allene moieties. Note that for each of the TS structures there are varying numbers of (*Z*)/(*E*) or *cis*/*trans* isomers, resulting in an overall number of 24 possible TSs.

Interestingly, **TS1** does not lead to the expected five-membered metallacycle, but yields instead an octahedral Rh(III) complex **INT2**, containing an η^3-allyl-η^1-allyl ligand (see Figure 2 for structure).[19] In what follows, we will refer to this kind of intermediate as η^3,η^1-bis(allylic), in accordance with the literature.[20] The formation of **INT2** is exergonic by 19.6 kcal/mol relative to **INT1**. This kind of η^3,η^1-bis(allylic) ligand could be expected to undergo *syn-anti* isomerization of the methyl substituents. However, intermediate **INT2** possesses some unique features that result in

the preservation of its stereochemical configuration as formed in the course of **TS1**, i.e. (*Z*)-double bond geometry and *anti*-CH_3 group in the η^3-allyl system. First, the methyl substituent in the η^3-allyl of **INT2** cannot move from *anti*- to *syn*-position via an η^3-η^1-η^3 isomerization mechanism, because the required rotation in the transient η^1-complex is impossible due to the fact that the allylic system is a part of metallacycle. Second, it is possible that the η^3 and η^1 allyl groups in **INT2** exchange places, but this also maintains the overall configuration. During such a process, the *anti*-CH_3 group becomes a substituent of the (*Z*)-configured double bond, and *vice-versa*. Finally, **INT2** may transiently transform into an isomeric η^3,η^1-bis(allylic) complex (**INT2'**). This is calculated to be 8.5 kcal/mol higher in energy than **INT2**. However, such an interconversion also leaves the stereochemical arrangement of the allene-dimer moiety intact. These properties are of importance for the overall selectivity of the reaction, as will be discussed below.

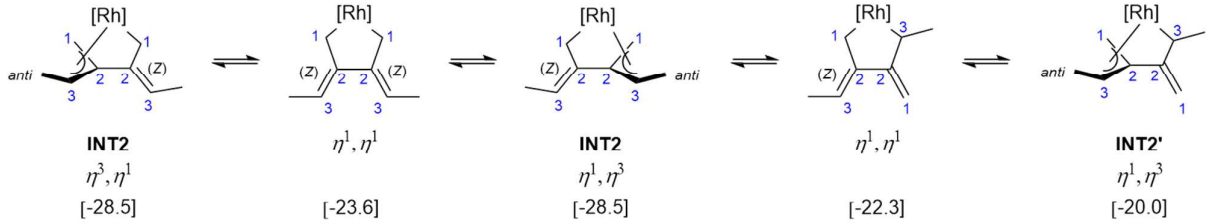

Scheme 5. Possible η^3-η^1-η^3 isomerization of **INT2**. Energies relative to the global zero are indicated in kcal/mol.

As a final option for the initial step, the oxidative coupling between the aldehyde and allene molecules was also examined (path C in Scheme 3). Similarly as in the case of allene-allene oxidative coupling, the C-C bond may be formed between the carbonyl carbon and positions C1, C2, or C3 of the allene. Considering also the Rh coordination, as well as the (*Z*)/(*E*) and *cis*/*trans*

isomers, there are 7 different transition states possible (see Supporting Information). The one with the lowest free energy among them is **TS1b** (Figure 2). The corresponding free energy barrier is 29.7 kcal/mol and formation of the resulting Rh(III) complex **INT2b** is endergonic by 8.7 kcal/mol relative to **INT1** (Figure 1).

These results clearly point to the oxidative coupling of two allenes leading to intermediate **INT2** as the favored initial step of the mechanism. The transition state for the C-H oxidative addition (**TS1a**) is 3.7 kcal/mol higher than **TS1** (but lower than many of the transition states depicted in Scheme 4). On the other hand, the oxidative coupling between the aldehyde and allene was found to occur via high-energy transition states, the lowest of which (**TS1b**) being 8.2 kcal/mol higher than **TS1**. Importantly, formation of **INT2** is irreversible, and therefore, already at this point it is possible to dismiss the whole paths A and C of Scheme 3 as plausible reaction mechanisms. Using the same argument one can also discard all the pathways starting with the oxidative coupling of two allenes in the other arrangement than in **TS1** (Scheme 4). Hence, from the reaction mixture containing the Rh(I) catalyst (**cat**), aldehyde **1**, and allene **2**, intermediate **INT2** should be formed practically exclusively. This intermediate, as explained above, has a defined stereochemical configuration, which strongly narrows the number of possible final products of the reaction.

In the following sections, we will show that the experimentally observed product **3**, as well as the minor side-products **4** and **5**, can all be derived from **INT2** as a common precursor.

3.2. Formation of the second C-C bond.

Once the two allene molecules are coupled in the first step of the mechanism forming **INT2**, the second C-C bond-formation must take place, incorporating the aldehyde moiety into the structure

and thus assembling the complete backbone of the product. It has been suggested that the second C-C bond-formation should occur via a migratory insertion of aldehyde into the Rh-C bond.[6] Such a course of the reaction was also established in mechanistic studies on the above-mentioned related reductive 2:1 coupling of acetylenes with aldehydes (Scheme 2a).[9] In addition to the insertion of the aldehyde, **INT2** may potentially undergo a competing process, namely a β-hydride elimination that would eventually lead to the formation of the dimer of allene **2**. There is experimental evidence that the latter pathway is followed in the absence of aldehyde **1** in the reaction mixture.[10] In the present study we discovered an additional alternative for the C-C bond formation that has not been proposed previously and that turns out to have a much lower barrier than the two other processes. It involves namely the direct rhodiumallyl addition to the aldehyde. In this section, these mechanistic possibilities are investigated and compared.[21]

Irrespective of the specific way the new C-C bond is formed, the reaction begins with the coordination of aldehyde **1** to the rhodium center. To create the necessary coordination site for the aldehyde, the allyl ligand must change its binding mode from η^3 to η^1. This may occur in two distinct ways, with either C1 or C3 ligating the metal center in the resulting complex (**INT3** or **INT3'**, respectively; Figure 3). This transformation is calculated to be endergonic by 4.1 and 6.7 kcal/mol, respectively.

From **INT3** the migratory insertion may only occur at the C1 position, due to the symmetric structure of this intermediate, while insertion in **INT3'**, on the other hand, can take place at both C1 and C3. The calculations show that the lowest energy transition state leads to the insertion at C1 (**TS-INS**) and arises from **INT3**. The second lowest transition state found is **TS-INS'**, which involves the insertion at C3 from **INT3'**. The corresponding barriers for **TS-INS** and **TS-INS'**

relative to **INT2** are 29.8 and 31.7 kcal/mol, respectively (Figure 3). The energy difference between them can be explained by the steric repulsion between the proximal methyl group and the aldehyde in the latter transition state.

The alternative C-C bond formation pathway that we discovered to be possible starting from **INT3** and **INT3'** is a direct attack of the σ-allyl ligand on the aldehyde, which is coordinated to the rhodium center.[22] Such a reaction, occurring via a six-membered cyclic transition state (see Figure 3 for a schematic picture and Figure 4 for optimized structures), was found to be energetically more favorable compared to the migratory insertion, by as much as 15 kcal/mol.

In this case, the C-C bond formation from **INT3** can now occur only at the C3 position (**TS2**). The corresponding barrier was calculated to be 14.7 kcal/mol relative to **INT2**. However, allylation from **INT3'** may take place at both C1 and C3, but the former scenario is lower in energy (**TS2'** in Figure 3) and requires overcoming an overall barrier of 15.3 kcal/mol relative to **INT2**. In both **TS2** and **TS2'** the six-membered ring adopts the chair-like geometry (Figure 4), with the methyl and the phenyl groups occupying the axial and equatorial positions, respectively. The small energy difference between them might be explained by a steric repulsion between the methyl group and the Rh center in **TS2'**, which is not present in **TS2**. Transition states **TS2** and **TS2'** constitute the divergence point, from which the reaction proceeds in two separate parallel pathways.

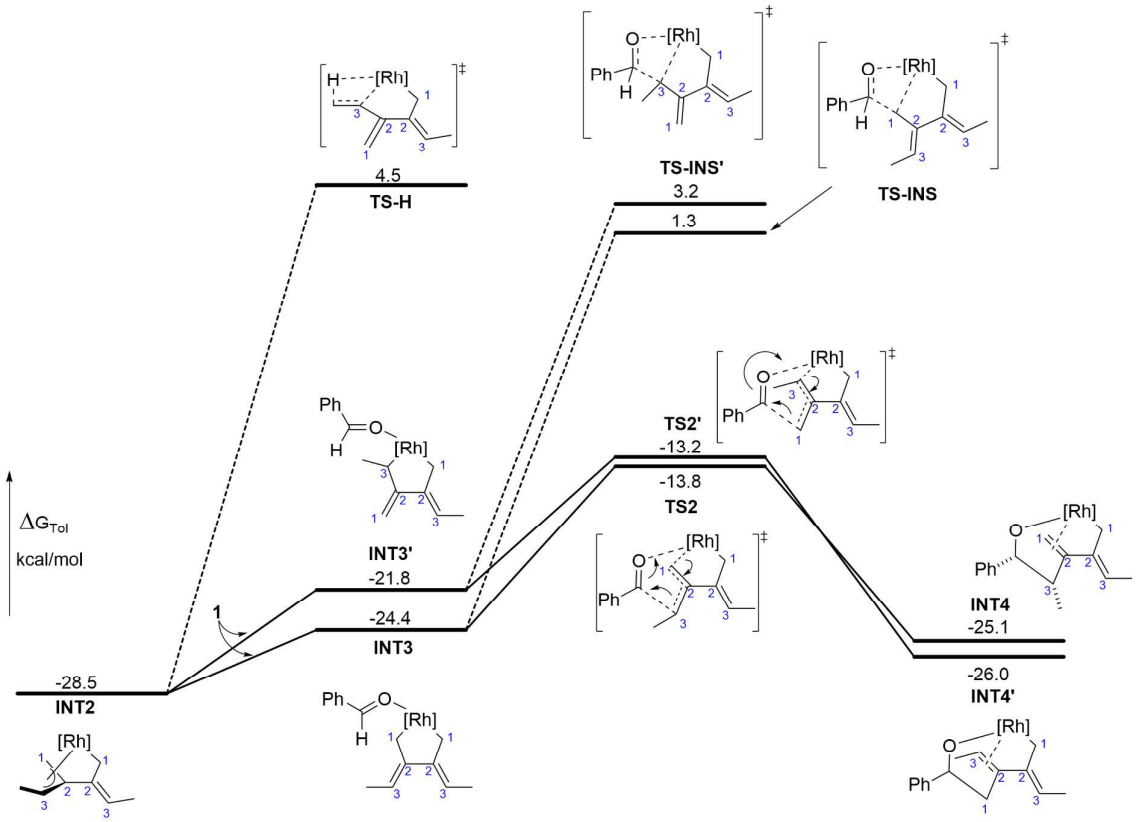

Figure 3. Free energy profile for the formation of the second C-C bond.

The allylation occurring via **TS2** and **TS2'** yields octahedral complexes **INT4** and **INT4'**, respectively, containing η^2-alkene and alkoxide ligands coordinated to Rh(III) (see Figure 4 for optimized structures). Interestingly, **INT4** is found to be 0.9 kcal/mol less stable than **INT4'**.

Finally, the β-hydride elimination from **INT2**, the possible side-reaction at this stage of the mechanism, was found to have a barrier of 33.0 kcal/mol relative to **INT2** (via **TS-H**, the optimized structure is given in Supporting Information), that is 18.3 kcal/mol higher than that found for **TS2** (Figure 3). Therefore, in the presence of aldehyde **1** in the reaction mixture, the allylation is expected to occur much more favorably, which is in agreement with the experimental results.

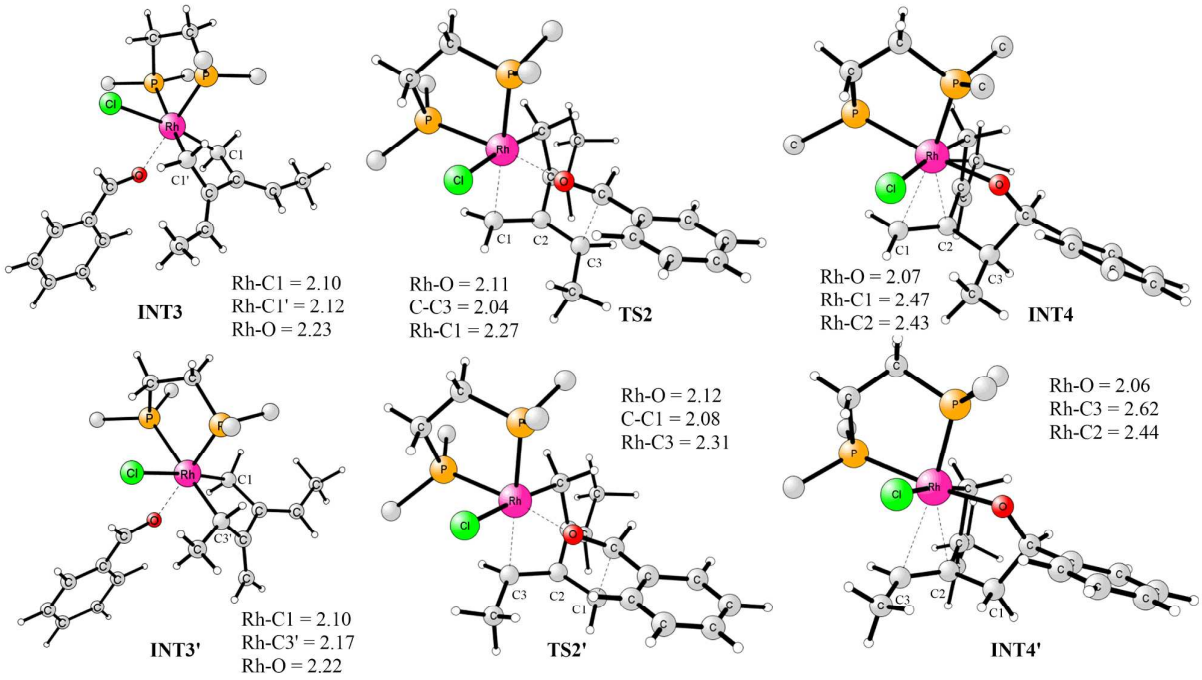

Figure 4. Optimized structures of the allylation reactants, transition states and the resulting complexes.

3.3. *β*-Hydride Elimination.

The next step in the reaction pathway is the *β*-hydride elimination, restoring the carbonyl group (Scheme 3, path B). In both **INT4** and **INT4**' the only *β*-hydrogen available is the one originating from the aldehyde group, hence it will be exclusively transferred to the metal center. However, for the *β*-hydride elimination to take place, a vacant coordination site must be created to accommodate the hydride. This can be generated by dissociation of the η^2-alkene from the metal center in **INT4** and **INT4**' followed by rotation of the alkoxide ligand. The calculations show that this isomerization takes place through a series of steps, among which the highest energy transition states are **TS3** and **TS3'** with the corresponding barriers of 17.7 and 16.6 kcal/mol relative to **INT4** and **INT4'**, respectively (Figure 5). A detailed description of the isomerization process, together with

calculated energy profiles and optimized structures can be found in the Supporting Information.

The isomerization results in intermediates **INT5** and **INT5'** containing η^3-allyl ligand, which are calculated to be higher in energy by 6.8 and 4.7 kcal/mol relative to **INT4** and **INT4'**, respectively. From **INT5** and **INT5'**, the β-hydride elimination takes place with a simultaneous change in the coordination mode of the allyl group from η^3 to η^1, in order to create a vacant site for the hydride at the metal center (**TS4** and **TS4'**, see Figure 6 for optimized structures). The calculated energies of **TS4** and **TS4'** relative to the respective intermediates **INT5** and **INT5**' are 9.0 and 10.1 kcal/mol (Figure 5), respectively. It should be noted that transitions states **TS4** and **TS4'** are lower in energy than the preceding **TS3** and **TS3'**, which will be of importance for the analysis of the selectivity (see below). The rhodium-hydride complexes resulting from the β-elimination (**INT6** and **INT6'**) are octahedral and contain an η^1-allyl and a carbonyl oxygen coordinated to the metal.

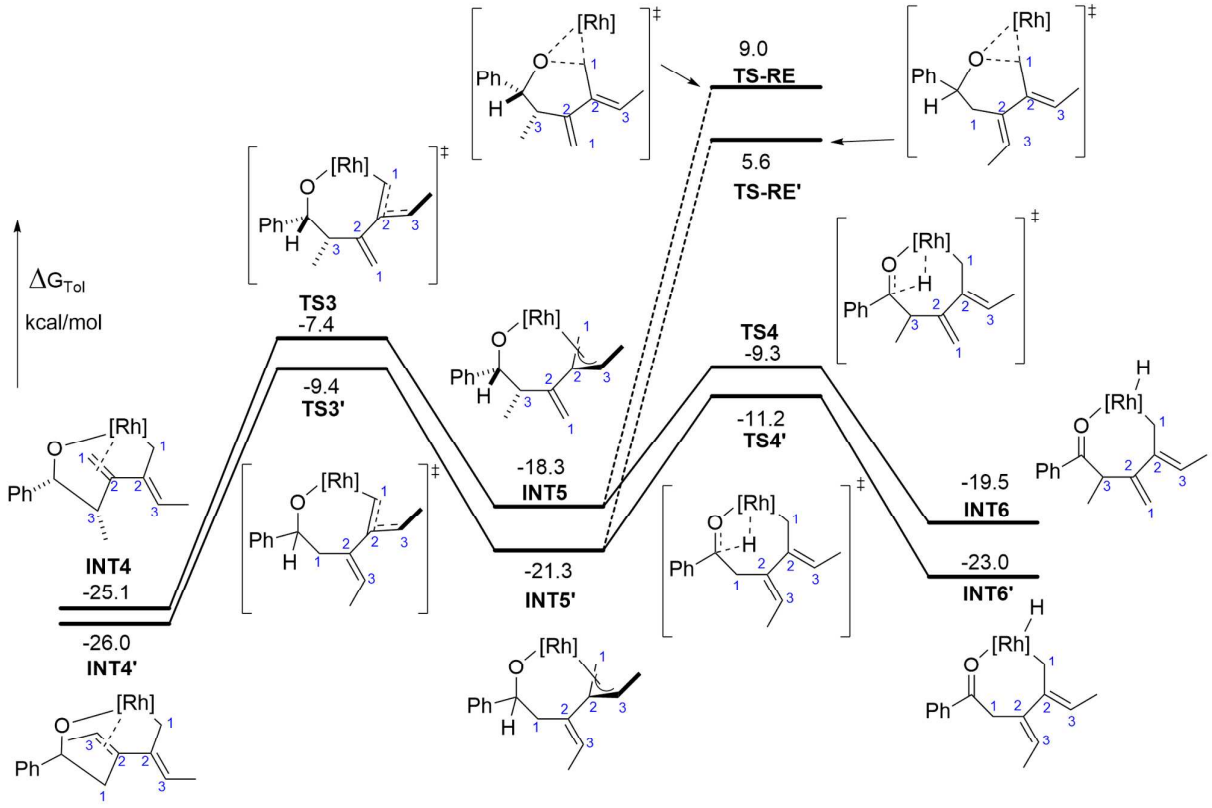

Figure 5. Free energy profile for the β-hydride elimination step.

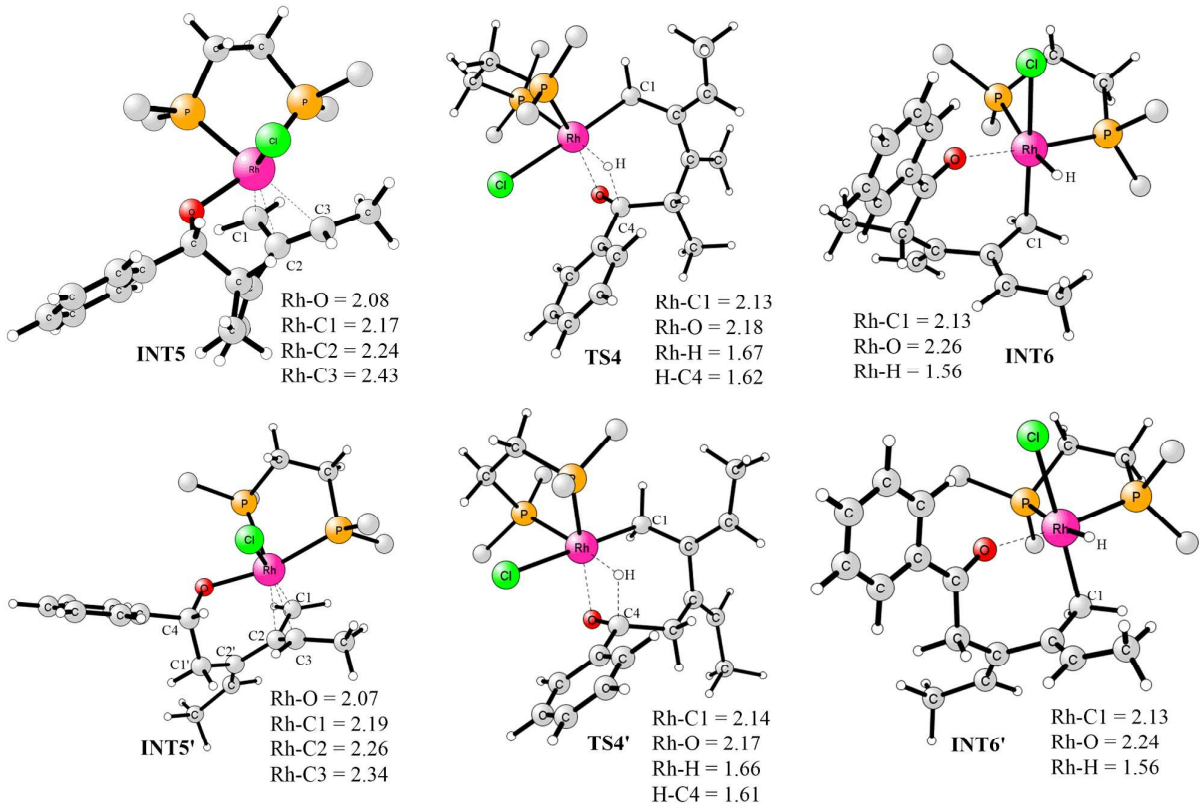

Figure 6. Optimized structures of the *β*-hydride elimination transition states and the resulting η^1-allyl complexes.

We have also considered an alternative process that theoretically may interfere with the *β*-hydride elimination from **INT5** or **INT5'**, that is a C-O bond forming reductive elimination. With such course, the reaction would yield pyrane derivatives as products, constituting a heteroatom analog of the [2+2+2] carbocyclization shown in Scheme 1a.[23] However, the barrier calculated for this process (from **INT5'** to **TS-RE'**) was found to be 26.9 kcal/mol, which is 16.8 kcal/mol higher than for the *β*-elimination from the same intermediate (Figure 6). Hence, the C-O bond forming reductive elimination will not take place, which is indeed the result observed experimentally.

3.4. Reductive Elimination.

The last step of the mechanism, closing the catalytic cycle, is the C-H bond-forming reductive elimination (Scheme 3). This could occur directly from **INT6** and **INT6'**. The calculated energy barriers are quite feasible, 20.4 and 19.2 kcal/mol from **INT6** and **INT6'**, respectively (see Supporting Information for optimized structures of TSs). However if the reaction followed this pathway, it would yield only compounds **4** and **5** as products, and not the experimentally-observed mixture containing predominantly their isomer **3**. Prompted by this apparent flaw, we envisioned that the η^1-allylic complexes **INT6** and **INT6'** could interconvert into their η^3-allylic counterparts (**INT7** and **INT7'**), with the dissociation of the carbonyl oxygen from the rhodium center prior to the reductive elimination. Since both terminal carbon atoms of the η^3-allyl system in **INT7** and **INT7'** can couple with the hydride during the reductive elimination, formation of **3** could be enabled upon such a transformation.

Indeed, as shown in Figure 7, the Rh(III) hydrides containing the η^3-allyl ligand, **INT7** and **INT7'** (see Figure 8 for structures), are more stable than **INT6** and **INT6'**, by 1.1 and 5.3 kcal/mol, respectively.[24] As mentioned above, from **INT7** and **INT7'** the reductive elimination can occur at both the C1 and C3 sides of the η^3-allyl. The calculations show that irrespective of the starting complex, the reductive elimination engaging the methyl-substituted carbon C3 (**TS5a** and **TS5a'**) is more favorable than the one occurring at the unsubstituted C1 (**TS5b** and **TS5b'**; Figure 8). This is a typical behavior in many Rh-catalyzed reactions involving π-allyl species, which usually afford the branched product.[19a-m] One reason for this preference is that in **TS5a** and **TS5a'** the sterically crowded rhodium center is positioned closer to the less substituted double bond (between C1 and C2). For example, in **TS5a'**, the bond distances of Rh-C1 and Rh-C2 are 2.15 and 2.16 Å, respectively, whereas in **TS5b'**, due to the steric effect of methyl group, the Rh-C2 and Rh-C3 bond

distances are somewhat longer, 2.19 and 2.22 Å, respectively (Figure 8). Importantly, the energies of all the **TS5** variants are lower than those of the transition states for the direct reductive elimination from **INT6** and **INT6'**, implying that the reaction will not follow the latter pathway.[25] The influence of the relative energies of the reductive elimination transition states on the overall selectivity of the reaction will be discussed in the following section.

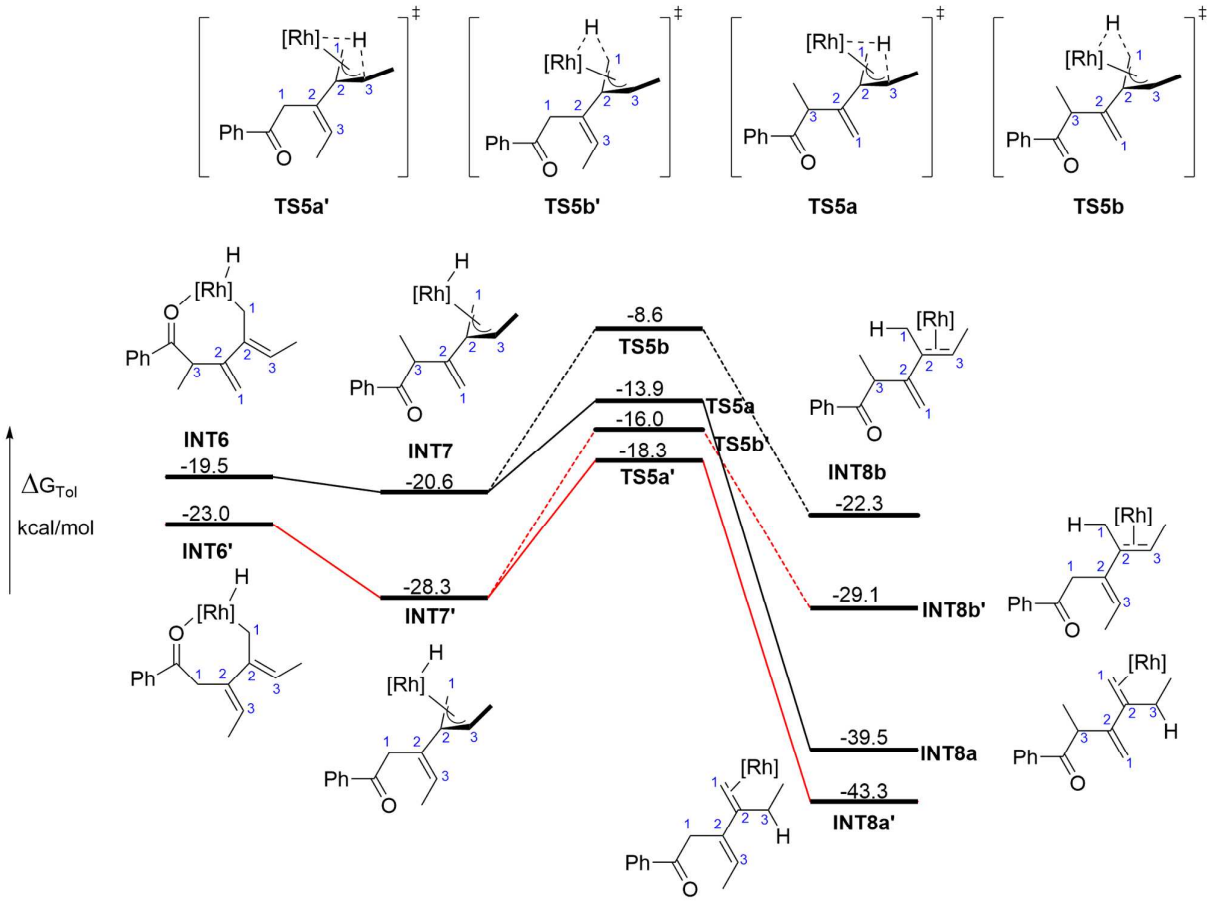

Figure 7. Free energy profile for the reductive elimination step.

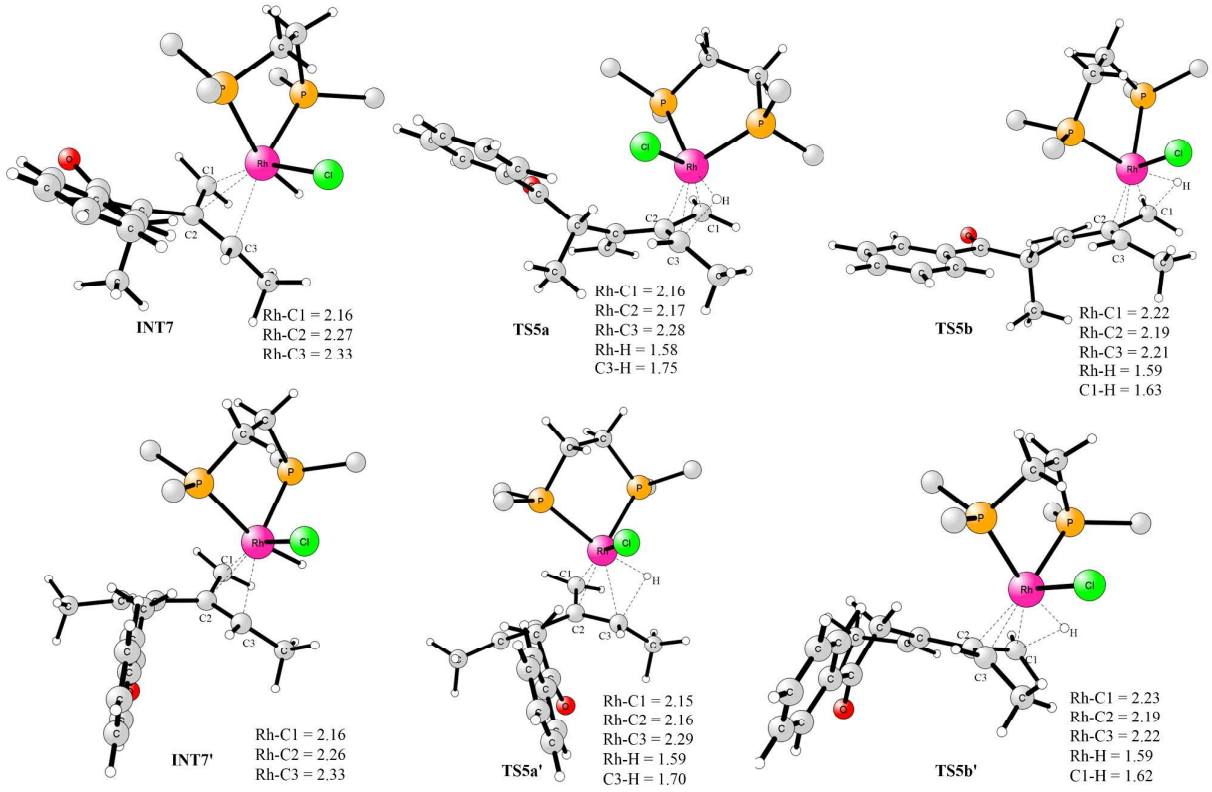

Figure 8. Optimized structures of the reductive elimination reactants and transition states.

3.5. Overall catalytic cycle and origins of regioselectivity in [RhCl(dppe)]-catalyzed reaction.

The mechanism of the reaction, as established by the present DFT calculations, is summarized in Scheme 6 and the corresponding overall free energy profile is given in Figure 9. The catalytic cycle consists of four steps: 1) oxidative coupling of two allene molecules, 2) allylation of the aldehyde, 3) *β*-hydride elimination, and 4) C-H forming reductive elimination. A prominent role in the mechanism is played by allylic Rh-complexes. Due to flexibility of the allyl ligand binding modes (η^3, η^1), a variety of reactivity patterns at each step of the catalytic cycle are available. Hence, the mechanism of the reaction involving allenes displays considerable differences compared to the mechanism of the related reductive coupling of acetylene and aldehyde shown in Scheme 2a,[9] in which vinyl ligands limited only to σ-bonding are involved.

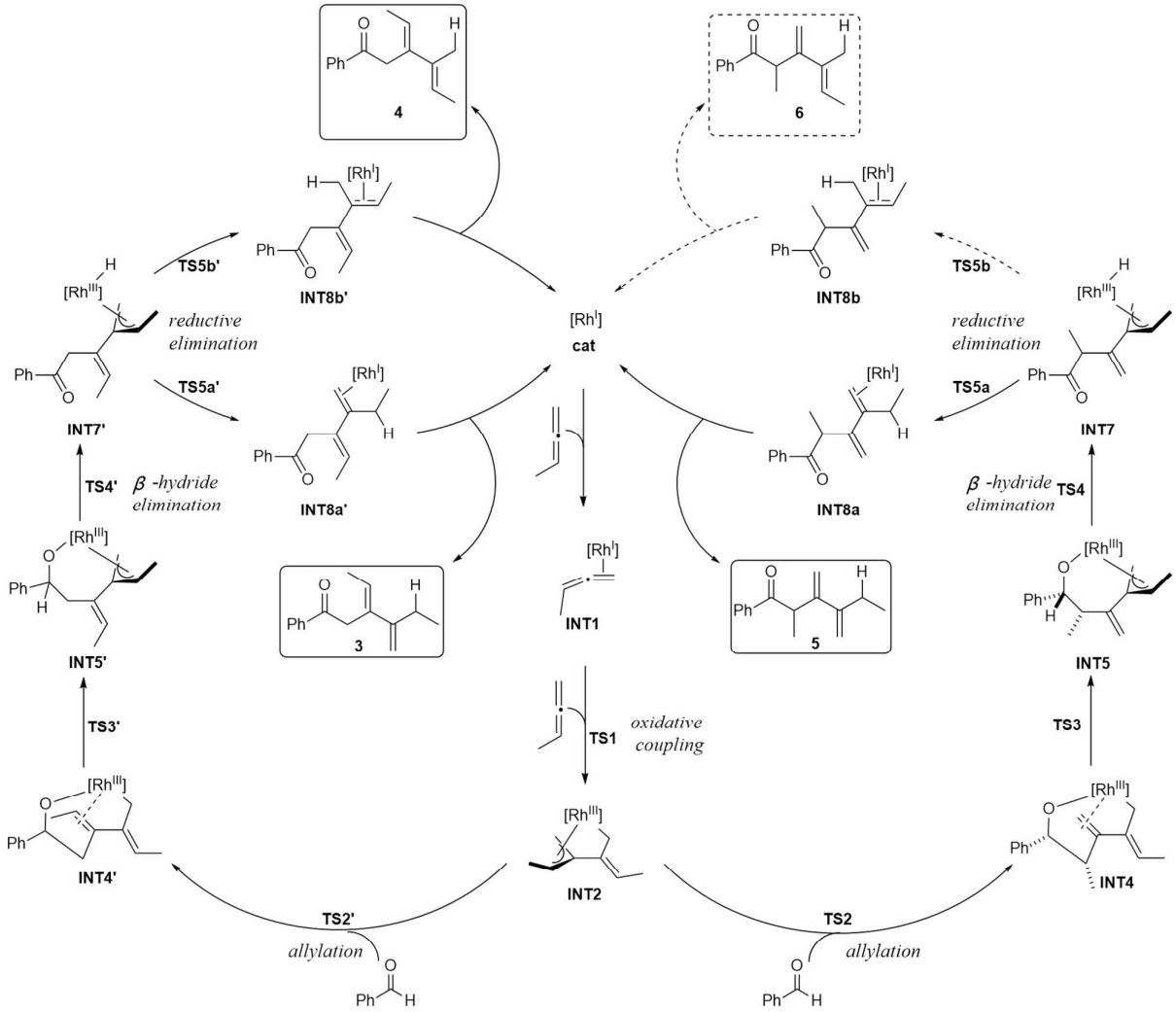

Scheme 6. Summary of the mechanism of the [RhCl(dppe)]-catalyzed 1:2 coupling of aldehydes and allenes.

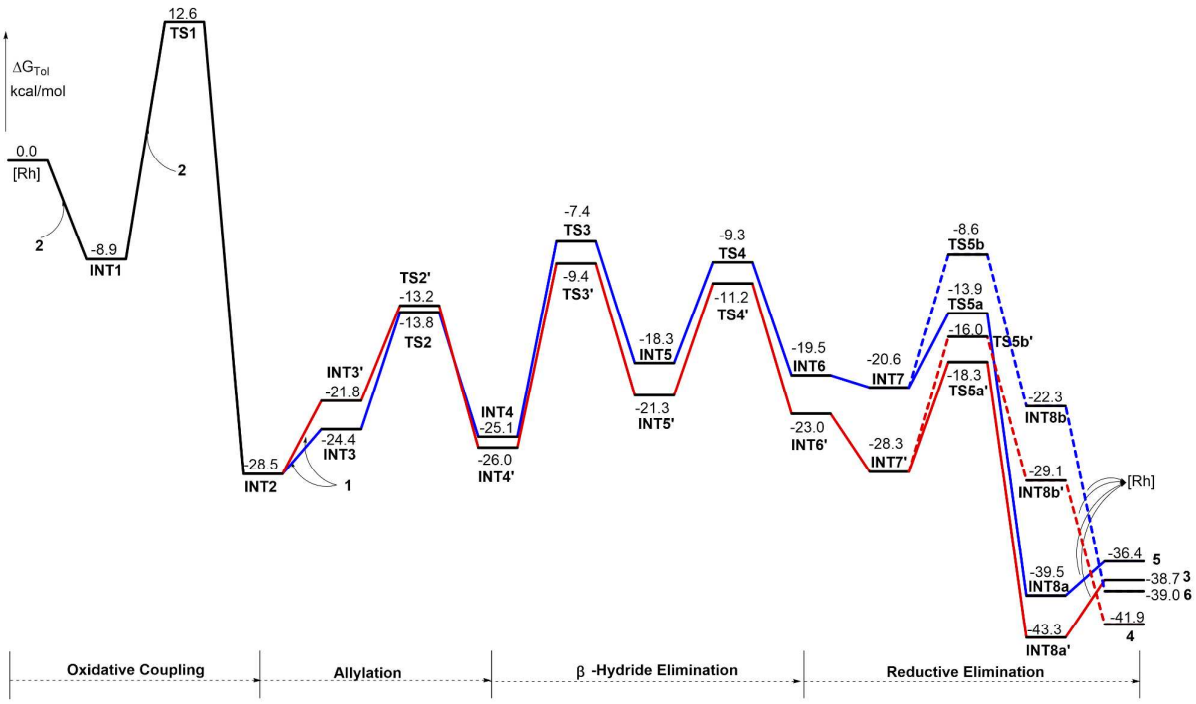

Figure 9. Free energy profile for the [RhCl(dppe)]-catalyzed 1:2 coupling of aldehydes and allenes.

The oxidative coupling of two allene molecules (**TS1**) is a common step for all the pathways leading to the experimentally observed products **3-5**. It has a barrier of 21.5 kcal/mol relative to the most stable Rh(I) complex **INT1**. The oxidative coupling is irreversible and leads selectively to the octahedral η^3,η^1-bis(allylic) Rh(III) complex **INT2**, which has a well-defined and stable stereochemical configuration. Therefore, at this step of the mechanism a number of structural features of the products are already determined, such as the C2-C2 linkage and the configuration of the double bonds. It is also important to point out that the overall barrier for the oxidative coupling is the highest among all the barriers in the catalytic cycle. This step constitutes therefore the rate-determining step of the reaction.

Upon coordination of an aldehyde molecule, **INT2** undergoes a transformation to either **INT3** or **INT3'**, depending on which side of the η^3-allyl ligand remains bound to the metal (C1 or C3). Thus,

this step constitutes the first divergence point, from which the two pathways proceed through the subsequent steps separately. The following step is the allylation of the aldehyde, proceeding through the six-membered cyclic transition states **TS2** and **TS2'**. After an isomerization (**INT4** → **INT5** via **TS3** and **INT4'** → **INT5'** via **TS3'**) required for creating an empty coordination site in an appropriate position of the complex, a *β*-hydride elimination takes place via **TS4** and **TS4'**. Since **TS3** and **TS3'** are higher in energy than all the subsequent transition states, passing them can be considered practically irreversible. Therefore, the ratio at which the catalyst is split to follow either one or the other branch of the catalytic cycle is determined by the energy difference between the transition states **TS3** and **TS3'**. According to the calculation, these energies differ by 2.0 kcal/mol, and hence intermediates **INT6** and **INT6'** are formed in a 5:95 ratio.[26]

The next step of the mechanism is the C-H forming reductive elimination, starting by converting the η^1-allylic Rh(III) hydrides **INT6** and **INT6'** to the η^3-allylic species **INT7** and **INT7'**, respectively. The reductive elimination is the final regioselectivity-determining step. This process was found to take place preferentially at the C3 position (**TS5a** and **TS5a'**) compared to C1 (**TS5b** and **TS5b'**). In particular, from **INT7'**, formation of **INT8a'** via **TS5a'** is favored over **INT8b'** via **TS5b'** by 2.3 kcal/mol. This energy difference corresponds approximately to a 98:2 ratio. On the other hand, the 5.3 kcal/mol energy difference between **TS5a** and **TS5b** implies that **INT7** is practically exclusively transformed into **INT8a**. Hence, taking into account the previous split of the reaction pathways, the overall selectivity predicted by the calculations is **3**:**4**:**5**/93:2:5, which is in a very good agreement with the experimentally-observed ratio of 91:6:3 (Scheme 2b).[6]

Finally, intermediates **INT8a'**, **INT8b'**, and **INT8a** formed in the reductive elimination regenerate the free catalyst [RhCl(dppe)] by releasing the corresponding products **3**, **4**, and **5**,

respectively, closing the catalytic cycle. It should be pointed out that the relative stabilities of the free products **3**, **4**, and **5** do not correlate at all with their ratios resulting from the catalyzed reaction.

In summary, the above considerations show that the calculated energies can reproduce and rationalize the observed selectivity of the [RhCl(dppe)]-catalyzed reaction, which provides further support to the reaction mechanism suggested in Scheme 6.

3.6. Regioselectivity in [Rh(dppe)$^+$]-catalyzed reaction.

As mentioned in the introduction, the selectivity of the reaction can be altered by replacing the chloride anion in the catalyst precursor with non-coordinating counterions, such as TfO^-, BF_4^-, or PF_6^-. To rationalize this catalyst-dependent selectivity, we have reinvestigated the reaction mechanism with the cationic [Rh(dppe)$^+$] complex as the active species. The calculations suggest that the cationic catalyst promotes a partially different mechanistic pathway (see Scheme 7 and Figure 10 for calculated energy profile), which in turn causes the alteration of the selectivity.

The first two steps of the mechanism are the same as for the [RhCl(dppe)] catalyst, except for the fact that due to the availability of an extra coordination site in the cationic catalyst, the initial **INT1**$^+$ complex contains two allene molecules. The reaction starts by an oxidative coupling of the two allene moieties (**TS1**$^+$), resulting in the selective formation of η^3,η^1-bis(allylic) complex **INT2**$^+$. The structure of the allylic ligand in **INT2**$^+$ is identical to that in **INT2**, limiting thus the possible reaction products to **3-6**, as discussed above for the neutral [RhCl(dppe)] catalyst. It should be noted that this step is rate-determining also for this catalyst. The next step is the allylation of the aldehyde via **TS2**$^+$ and **TS2'**$^+$, resulting in intermediates **INT4**$^+$ and **INT4'**$^+$. The selectivity of the allylation

is the same as before, i.e. it occurs preferentially at the C3 position via **TS2**$^{+}$.

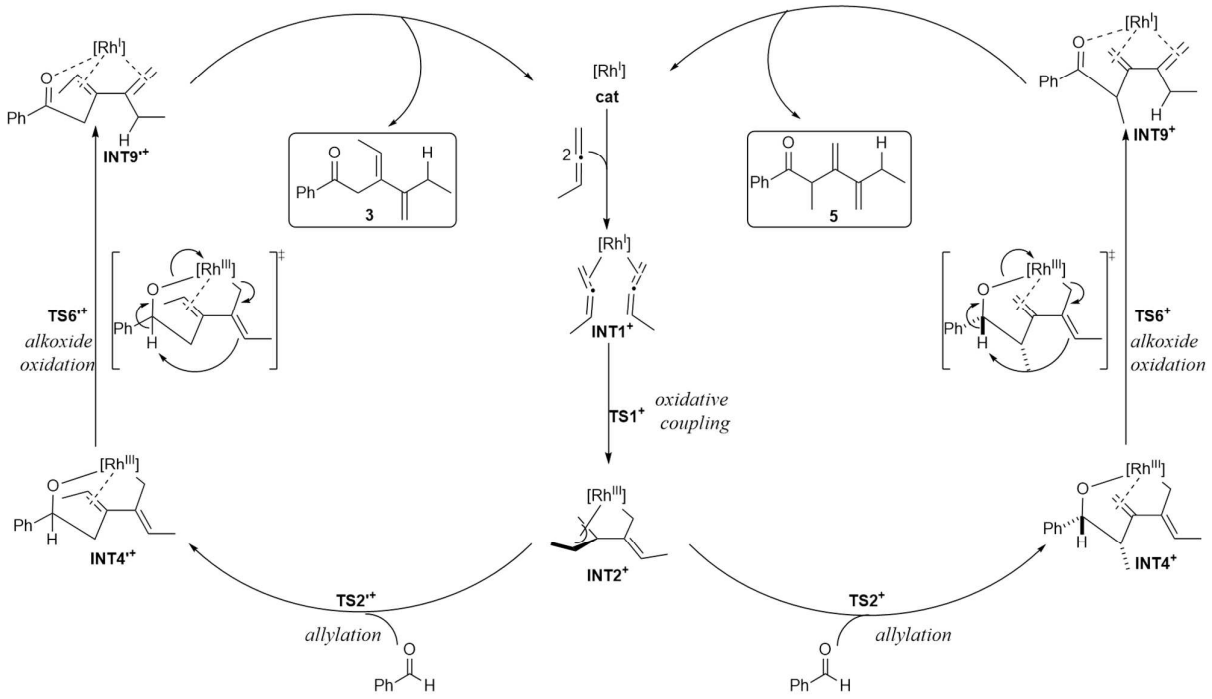

Scheme 7. Summary of the mechanism of the [Rh(dppe)$^{+}$]-catalyzed 1:2 coupling of aldehydes and allenes.

From **INT4**$^{+}$ and **INT4'**$^{+}$, the reaction can follow the same isomerization/*β*-hydride elimination/reductive elimination pathway found for the neutral catalyst. The optimized geometries and the calculated energy profile for this scenario are given in the Supporting Information. Similarly to the neutral catalyst, the highest barrier is calculated to be for the isomerization (**TS3**$^{+}$ and **TS3'**$^{+}$), amounting to 12.0 and 12.2 kcal/mol relative to **INT4**$^{+}$ and **INT4'**$^{+}$, respectively. However, although the energy barriers are feasible, if such analogous pathway is followed it would lead to the same selectivity as before, i.e. predominantly product **3** (see SI). This is in conflict with the experimental findings, which speaks thus against such a mechanism for the cationic catalyst.

Instead, we discovered an alternative mechanism which reproduces the reversed selectivity in the cationic catalyst. The alkoxide ligand present in the Rh(III) complexes **INT4**$^+$ and **INT4'**$^+$ can namely undergo a feasible direct oxidation to the corresponding ketone (**TS6**$^+$ and **TS6'**$^+$, see Figure 11 for optimized structures). In the course of the reaction, Rh(III) is reduced to Rh(I) and the final products **3** and **5** are formed directly (coordinated to the metal as **INT9'**$^+$ and **INT9**$^+$). A key role in this process is played by the η^1-allyl ligand, which acts as an internal base abstracting a proton from the alkoxide (Figure 11). Although perhaps somewhat surprising in this context, this transformation is analogous to the well-known oxidation of alcohols by high-valent metals, such as for example Mn(VII) and Cr(VI).[27] The example of related oxidation in Pd(II) complexes has also been reported.[28]

The barriers for **TS6**$^+$ and **TS6'**$^+$ relative to **INT4**$^+$ and **INT4'**$^+$ are calculated to be 10.1 and 12.0 kcal/mol, respectively. As seen from the energy profile in Figure 10, the regioselectivity in this case is controlled by the energy difference between **TS2'**$^+$ and **TS6**$^+$, which constitute the first irreversible steps in the respective pathways leading to the two products. The calculated energy difference between these transition states is 0.3 kcal/mol, corresponding to a **3**:**5** ratio of 40:60.

Although the difference in energy barriers between the isomerization/β-hydride elimination/reductive elimination pathway (12.0 and 12.2 kcal/mol for **TS3**$^+$ and **TS3'**$^+$, respectively) and the alkoxide oxidation pathway (10.1 and 12.0 kcal/mol for **TS6**$^+$ and **TS6'**$^+$, respectively) is not that large that the former one can be completely ruled out, the fact that the alkoxide oxidation mechanism can account for the reversal of selectivity in the cationic catalyst is a strong argument in favor of it. Another piece of evidence is that the alkoxide oxidation via **TS6**$^+$ and **TS6'**$^+$ leads directly to compounds **3** and **5**, which explains why these are the only products

observed experimentally for the reaction involving the cationic catalyst, while for the neutral catalyst, on the other hand, three products were observed.

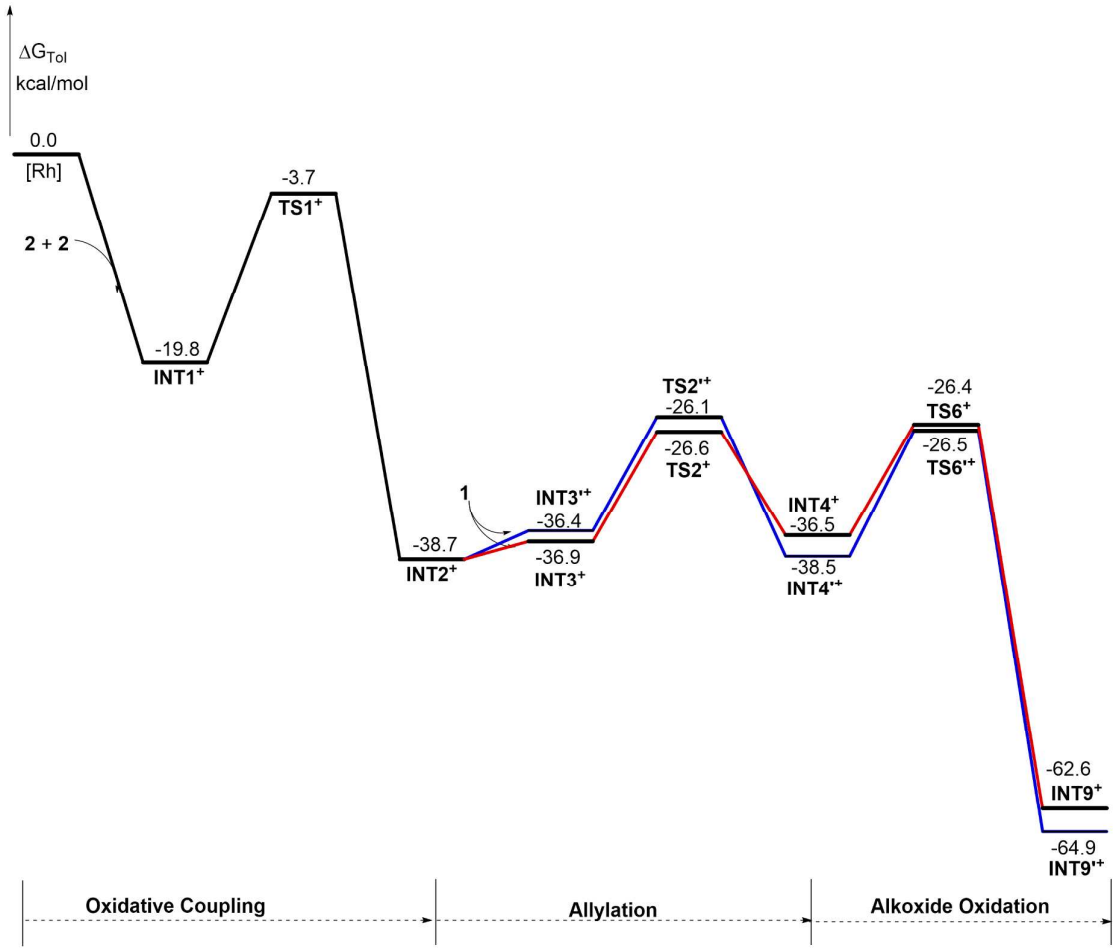

Figure 10. Free energy profile for the [Rh(dppe)$^+$]-catalyzed 1:2 coupling of aldehydes and allenes.

Finally, it should be mentioned that we also located transition states for a similar alkoxide oxidation mechanism in the chloride-containing neutral complexes **INT4** and **INT4'**. However, the barriers were found to be much higher than the isomerization/*β*-hydride elimination/reductive elimination pathway discussed above (see Supporting Information for details). Hence, the electron deficient character of rhodium in the cationic complex is crucial for the alkoxide oxidation reaction.

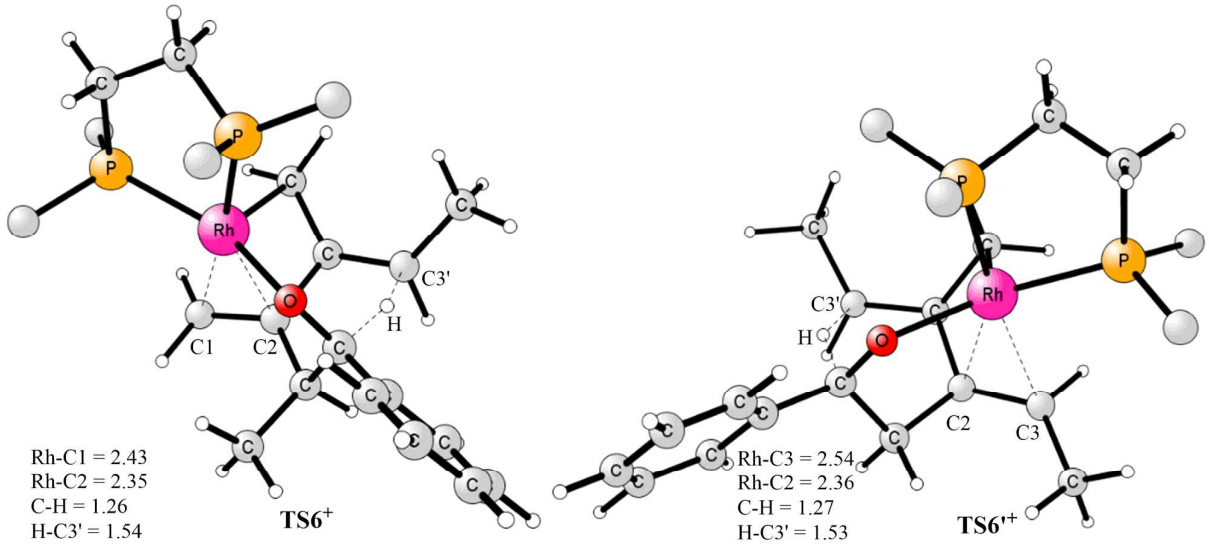

Figure 11. Optimized structures of the alkoxide oxidation transition states **TS6**$^{+}$ and **TS6'**$^{+}$.

4. Conclusions

The rhodium-catalyzed 1:2 coupling of aldehydes and allenes has been investigated in detail by DFT calculations. The free energy profiles for several possible reaction pathways are calculated and compared.

For the reaction catalyzed by the neutral [RhCl(dppe)] complex, it is shown that the energetically most plausible catalytic cycle consists of the following steps: oxidative coupling of the two allenes, allylation of the aldehyde, β-hydride elimination, and finally, reductive elimination. The first step is found to be rate-determining for the overall reaction and it leads to the formation of a Rh(III) bis(allylic) complex. Due to its ability to adopt either η^3 or η^1 configurations, the allyl ligand turns out to play a key role throughout the mechanism, with profound consequences for the reaction selectivity.

The calculations show that the remarkable regioselectivity of the reaction is an overall result of a number of selection events taking place in the catalytic cycle. The first regioselectivity-determining step is the oxidative coupling, at which the C2-C2 linkage between the allene moieties is selectively established. Subsequently, the selectivity of the second C-C bond formation is controlled during the β-hydride elimination. Finally the reductive elimination is found to preferentially yield the branched product.

For the reaction catalyzed by the cationic [Rh(dppe)$^+$] complex, on the other hand, the calculations suggest a different reaction mechanism after the allylation step. Namely, oxidation of the alkoxide can take place directly to yield the products. This important difference explains the reversal of selectivity observed experimentally.

The present calculations provide thus important insights into the mechanism of rhodium(I)-catalyzed coupling reactions, in particular those involving allenes, and will have a general bearing on the improvement of existing catalytic systems and the design of new ones.

Acknowledgment. We acknowledge financial support from the Swedish Research Council, the Göran Gustafsson Foundation and the Knut and Alice Wallenberg Foundation. G.H. thanks the Carl-Trygger Foundation for a postdoctoral fellowship. Computer time was generously provided by the Swedish National Infrastructure for Computing.

Supporting Information Available: Additional results not shown in the text and Cartesian coordinates of all optimized structures discussed in the paper. This material is available free of charge via the Internet at http://pubs.acs.org.

References

1. (a) Lautens, M.; Klute, W.; Tam, W., *Chem. Rev.* **1996**, *96*, 49-92; (b) Kotha, S.; Brahmachary, E.; Lahiri, K., *Eur. J. Org. Chem.* **2005**, *22*, 4741-4767; (c) Murakami, M., *Angew. Chem. Int. Ed.* **2003**, *42*, 718-720; (d) Inglesby, P. A.; Evans, P. A., *Chem. Soc. Rev.* **2010**, *39*, 2791-2805; (e) Shibata, T.; Tsuchikama, K., *Org. Biomol. Chem.* **2008**, *6*, 1317-1323; (f) Tanaka, K., *Chem.–Asian J.* **2009**, *4*, 508-518; (g) Yu, Z.-X.; Wang, Y.; Wang, Y., *Chem.–Asian J.* **2010**, *5*, 1072-1088.
2. (a) Willis, M. C., *Chem. Rev.* **2010**, *110*, 725-748; (b) Jun, C.-H.; Moon, C. W.; Lee, D.-Y., *Chem. Eur. J.* **2002**, *8*, 2422-2428; (c) Leung, J. C.; Krische, M. J., *Chem. Sci.* **2012**, *3*, 2202-2209.
3. (a) Jang, H.-Y.; Krische, M. J., *Acc. Chem. Res.* **2004**, *37*, 653-661; (b) Ngai, M.-Y.; Kong, J.-R.; Krische, M. J., *J. Org. Chem.* **2007**, *72*, 1063-1072; (c) Iida, H.; Krische, M. J., *Top. Curr. Chem.* **2007**, *279*, 77-104; (d) Bower, J. F.; Kim, I. S.; Patman, R. L.; Krische, M. J., *Angew. Chem. Int. Ed.* **2009**, *48*, 34-46; (e) Skucas, E.; Ngai, M.-Y.; Komanduri, V.; Krische, M. J., *Acc. Chem. Res.* **2007**, *40*, 1394-1401.
4. Kong, J. R.; Krische, M. J., *J. Am. Chem. Soc.* **2006**, *128*, 16040-16041.
5. The reaction scope was later expanded by inclusion of other aldehydes and imines as coupling partners. See: (a) Skucas, E.; Kong, J. R.; Krische, M. J., *J. Am. Chem. Soc.* **2007**, *129*, 7242-7243; (b) Han, S. B.; Kong, J. R.; Krische, M. J., *Org. Lett.* **2008**, *10*, 4133-4135.

6. Toyoshima, T.; Miura, T.; Murakami, M., *Angew. Chem. Int. Ed.* **2011**, *50*, 10436-10439.

7. (a) Oonishi, Y.; Hosotani, A.; Sato, Y., *J. Am. Chem. Soc.* **2011**, *133*, 10386-10389; (b) Hojo, D.; Tanaka, K., *Org. Lett.* **2012**, *14*, 1492-1495.

8. 36 refers only to the number of possible linear compounds containing the reactant molecules coupled in a aldehyde-allene-allene sequence. In fact, two of the above isomers contain two asymmetric carbon atoms and can hence exist as two diastereomers, raising the number of possible products with distinct energies to 38. If cyclic structures and those containing allene-aldehyde-allene sequence are also considered, the number of possible products is even greater.

9. Williams, V. M.; Kong, J. R.; Ko, B. J.; Mantri, Y.; Brodbelt, J. S.; Baik, M.-H.; Krische, M. J., *J. Am. Chem. Soc.* **2009**, *131*, 16054-16062.

10. Miura, T.; Biyajima, T.; Toyoshima, T.; Murakami, M., *Beilstein J. Org. Chem.* **2011**, *7*, 578-581.

11. In fact, to the best of our knowledge, all the transition metal catalyzed [n+m+o] cycloadditions involving allenes developed so far incorporate only one or two molecules of allene into the product. See: (a) Murakami, M.; Ubukata, M.; Itami, K.; Ito, Y., *Angew. Chem. Int. Ed.* **1998**, *37*, 2248-2250; (b) Shanmugasundaram, M.; Wu, M.-S.; Cheng, C.-H., *Org. Lett.* **2001**, *3*, 4233-4236; (c) Shanmugasundaram, M.; Wu, M.-S.; Jeganmohan, M.; Huang, C.-W.; Cheng, C.-H., *J. Org. Chem.* **2002**, *67*, 7724-7729; (d) Miura, T.; Morimoto, M.; Murakami, M., *J. Am. Chem. Soc.* **2010**, *132*, 15836-15838; (e) Brusoe, A. T.; Alexanian, E. J., *Angew. Chem. Int. Ed.* **2011**, *50*, 6596-6600.

12. (a) McCarren, P. R.; Liu, P.; Cheong, P. H.-Y.; Jamison, T. F.; Houk, K. N., *J. Am. Chem.*

Soc. **2009**, *131*, 6654-6655; (b) Liu, P.; McCarren, P.; Cheong, P. H.-Y.; Jamison, T. F.; Houk, K. N., *J. Am. Chem. Soc.* **2010**, *132*, 2050-2057; (c) Liu, P.; Krische, M. J.; Houk, K. N., *Chem. Eur. J.* **2011**, *17*, 4021-4029.

13. *Gaussian03*, Revision D.01, Frisch, M. J., et al. Gaussian, Inc., Wallingford CT, 2004.
14. (a) Becke, A. D., *J. Chem. Phys.* **1993**, *98*, 5648-5652; (b) Lee, C. T.; Yang, W. T.; Parr, R. G. *Phys. Rev. B* **1988**, *37*, 785-789.
15. Hay, P. J.; Wadt, W. R., *J. Chem. Phys.* **1985**, *82*, 270-283.
16. (a) Barone, V.; Cossi, M., *J. Phys. Chem. A* **1998**, *102,* 1995-2001; (b) Cossi, M.; Rega, N.; Scalmani, G.; Barone, V., *J. Comput. Chem.* **2003**, *24*, 669-681.
17. Grimme, S., *J. Comput. Chem.* **2006**, *27*, 1787-1799.
18. See for instance: (a) Minenkov, Y.; Occhipinti, G.; Jensen, V. R., *J. Phys. Chem. A* **2009**, *113*, 11833-11844; (b) Siegbahn, P. E. M.; Blomberg, M. R. A.; Chen, S.-L., *J. Chem. Theory Comput.* **2010**, *6*, 2040-2044; (c) Harvey, J. N., *Faraday Discuss*. **2010**, 145, 487-505; (d) McMullin, C. L.; Jover, J.; Harvey, J. N.; Fey, N., *Dalton Trans*. **2010**, *39*, 10833-10836; (e) Lonsdale, R.; Harvey, J. N.; Mulholland, A. J., *J. Phys. Chem. Lett*. **2010**, *1*, 3232-3237; (f) Osuna, S.; Swart, M.; Solà, M., *J. Phys. Chem. A* **2011**, *115*, 3491-3496; (g) Santoro, S.; Liao, R.-Z.; Himo, F., *J. Org. Chem*. **2011**, *76*, 9246-9252; (h) Nordin, M.; Liao, R.-Z.; Ahlford, K.; Adolfsson, H.; Himo, F., *ChemCatChem.* **2012**, *4,* 1095-1104; (i) Xu, X.; Liu, P.; Lesser, A.; Sirois, L. E.; Wender, P. A.; Houk, K. N., *J. Am. Chem. Soc.* **2012**, *134,* 11012-11025; (j) Jiménez-Halla, J. O. C.; Kalek, M.; Stawinski, J.; Himo, F., *Chem. Eur. J.* **2012**, *18*, 12424–12436; (k) Kalek, M.; Himo, F., *J. Am. Chem. Soc.* **2012**, *134,* 19159-119169; (l) Huang, G.; Xia, Y.; Sun, C.; Li, J.; Lee, D.,

J. Org. Chem. **2013**, *78*, 988-995.

19. For reports of η^3-allyl Rh species, see for example: (a) Evans, P. A.; Lawler, M. J., *J. Am. Chem. Soc.* **2004**, *126*, 8642-8643; (b) Evans, P. A.; Leahy, D. K., *Chemtracts*. **2003**, *16*, 567–578; (c) Evans, P. A.; Leahy, D. K.; Slieker, L. M., *Tetrahedron: Asymmetry.* **2003**, *14*, 3613–3618; (d) Evans, P. A.; Robinson, J. E.; Moffett, K. K., *Org. Lett.* **2001**, *3*, 3269-3271; (e) Arnold, J. S.; Cizio, G. T.; Nguyen, H. M., *Org. Lett.* **2011**, *13*, 5576–5579; (f) Arnold, J. S.; Cizio, G. T.; Heitz, D. R.; Nguyen, H. M., *Chem. Commun*. **2012**, *48,* 11531-11533; (g) Arnold, J. S.; Stone, R. F.; Nguyen, H. M., *Org. Lett*. **2010**, *12*, 4580–4583; (h) Arnold, J. S.; Nguyen, H. M., *J. Am. Chem. Soc.* **2012**, *134*, 8380-8383; (i) Hayashi, T.; Okada, A.; Suzuka, T.; Kawatsura, M., *Org. Lett*. **2003**, *5*, 1713–1715; (j) Vrieze, D. C.; Hoge, G. S.; Hoerter, P. Z.; Van Haitsma, J. T.; Samas, B. M., *Org. Lett*. **2009**, *11*, 3140–3142; (k) Koschker, P.; Lumbroso, A.; Breit, B., *J. Am. Chem. Soc.* **2011**, *133*, 20746-20749; (l) Lumbroso, A.; Koschker, P.; Vautravers, N. R.; Breit, B., *J. Am. Chem. Soc.* **2011**, *133*, 2386-2389; (m) Nishimura, T.; Hirabayashi, S.; Yasuhara, Y.; Hayashi, T., *J. Am. Chem. Soc.* **2006**, *128*, 2556-2557; (n) Choi, J.-c.; Osakada, K.; Yamamoto, T., *Organometallics* **1998**, *17*, 3044-3050; (o) Barros, H. J. V.; Guimarães, C. C.; dos Santos, E. N.; Gusevskaya, E. V., *Organometallics* **2007**, *26*, 2211-2218; (p) Jiao, L.; Lin, M.; Zhuo, L.-G.; Yu, Z.-X., *Org. Lett*. **2010**, *12*, 2528–2531; (q) Jiao, L.; Lin, M.; Yu, Z.-X., *J. Am. Chem. Soc.* **2011**, *133*, 447-461; (r) Lin, M.; Li, F.; Jiao, L.; Yu, Z.-X., *J. Am. Chem. Soc.* **2011**, *133*, 1690-1693; (s) Lin, M.; Kang, G.-Y.; Guo, Y.-A.; Yu, Z.-X., *J. Am. Chem. Soc.* **2012**, *134*, 398-405; (t) Li, Q.; Yu, Z.-X., *Organometallics* **2012**, *31*, 5185-5195.

20. (a) Szabó, K. J., *Chem. Eur. J.* **2004**, *10*, 5268–5275; (b) Szabó, K. J., *Chem. Eur. J.* **2000**, *6*, 4413–4421.

21. There is an additional possibility of a migratory insertion of a third molecule of allene instead of the aldehyde. Such a pathway would eventually lead to the [2+2+2] trimerization of the allene. However, since experimentally allene **2** only dimerizes (see ref. 10) this possibility was not considered computationally.

22. For selected reviews on allylation of carbonyl compounds, see: (a) Denmark, S. E.; Fu, J., *Chem. Rev.* **2003**, *103*, 2763-2794; (b) Kennedy, J. W. J.; Hall, D. G., *Angew. Chem., Int. Ed.* **2003**, *42*, 4732-4739; (c) Yu, C.-M.; Youn, J.; Jung, H.-K., *Bull. Korean Chem. Soc.* **2006**, *27*, 463-472; (d) Marek, I.; Sklute, G., *Chem. Commun.* **2007**,1683-1691; (e) Hall, D. G. *Synlett* **2007**, 1644-1655.

23. For examples of [2+2+2] cyclization involving carbonyl compounds, see: (a) Tsuchikama, K.; Yoshinami, Y.; Shibata, T., *Synlett* **2007**, 1395-1398; (b) Tanaka, K.; Otake, Y.; Wada, A.; Noguchi, K.; Hirano, M., *Org. Lett.* **2007**, *9*, 2203-2206.

24. Transition states connecting **INT6** to **INT7** and **INT6'** to **INT7'** could not be optimized. However, energy scans show the barriers are quite low, much lower than those for the direct reductive elimination (see Supporting Information).

25. The methyl group in the η^3-allyl complexes **INT7** and **INT7'**, contrary to the case of **INT2** discussed above, can undergo a relocation from *anti* to *syn* position. This could potentially lead to the formation of isomers of products **4** and **6**, containing different configurations at one of the double bonds. However, the barriers for the *syn-anti* substituent exchange in **INT7** and **INT7'** were calculated to be much higher than those

for the reductive elimination. Therefore, **INT7** and **INT7'** undergo the reductive elimination before they can isomerize. See Supporting Information for details.

26. The ratios are calculated using the Eyring equation. For example, the ratio of **INT6** and **INT6'** is calculated according to:

$$\frac{\mathrm{INT6}}{\mathrm{INT6'}} = e^{\frac{\Delta G_{Tol}(\mathrm{TS3}) - \Delta G_{Tol}(\mathrm{TS3'})}{RT}}$$

27. Wade, L. G. Jr., *Organic chemistry*, 6th ed.; Prentice-Hall: Upper Saddle River, NJ, 2006.

28. Nielsen, R. J.; Goddard III, W. A., *J. Am. Chem. Soc.* **2006**, *128*, 9651-9660.

TOC GRAPHICS